DERIVATION OF PM10 LEVELS USING OBRA ON LANDSAT 5 TM IMAGES: A CASE STUDY IN IZMIR, TURKEY

Emre Ozelkan[1], Muhittin Karaman[2,*], Suleiman Mostamandy[3], Z. Damla Uca Avci[4] and Hüseyin Toros[5]

[1] Istanbul Technical University, Agricultural and Environmental Informatics Application and Research Center, Maslak 34469, Istanbul, Turkey
[2] Istanbul Technical University, Geochemistry Research Group and JAL Laboratories, Maslak 34469, Istanbul, Turkey
[3] Russian State Hydrometeorological University, Maloohtinsky 98, St.Petersburg 195196, Russia
[4] Istanbul Technical University, Department of Astronautical Engineering, Maslak 34469, İstanbul, Turkey
[5] Istanbul Technical University, Department of Meteorological Engineering, Maslak 34469, İstanbul, Turkey

Presented at the 17th International Symposium on Environmental Pollution and its Impact on Life in the Mediterranean Region (MESAEP), September 28 - October 01, 2013, Istanbul, Turkey

ABSTRACT

Remote sensing is a convenient and promising technique in air quality management. It can be used to determine local and global spatial distribution of Particulate Matter (PM10) data. Determination of PM10 data using multispectral satellite images' reflectance values was the main aim of this study. For this purpose, 19.02.2010 and 26.03.2011 dated Landsat 5TM multispectral satellite images were used. The PM10 data of Izmir, a metropolitan city in Turkey, was also gathered from *in situ* air quality measurement stations. The highest, lowest and average PM10 values measured were 172, 92.5 and 124.4 μgm^{-3} on 19.02. 2010, and 64.5, 31 and 48.7 μgm^{-3} on 26.03. 2011, respectively. Difference images, that were obtained by subtraction of atmospheric corrected images from top of atmosphere reflectance (TOA) calculated images, were used in the study. Optimum Band Ratio (OBRA) method was used to produce all possible band ratio (BR) indices of the difference images. Additionally, the filter sizes from 1x1 (direct value of a station) to 11x11 were applied to generate difference images for determining the suitable filter size correlated ones with *in-situ* PM10 data. The results were correlated with PM10 values. The BR of 1650 nm centered Mid-IR 1 (band 5) and 2315 nm centered Mid-IR 2 (band 7) with 3x3 filter size was found to be suitable to determine PM10 data with remote sensing. The highest correlation coefficients between PM10 and the values of [band 5 (B5)/band 7 (B7)] and B7/B5 ratio indices were obtained as r = 0.86 for 19.02. 2010 and 26.03. 2011, respectively. The results show that the B5/B7 and B7/B5 ratio values of Landsat 5TM were more correlated and appropriate than other BRs to determine PM10. Additionally, the simulation of an online coupled regional meteorology-chemistry Enviro-HIRLAM model was run for the two dates. Model 45 h forecast results, being compatible with remote sensing results, indicated that the PM10 content in the region is higher on 19.02. 2010.

* Corresponding author

KEYWORDS: PM10, air pollution, remote sensing, Landsat 5 TM, OBRA, NWP

1. INTRODUCTION

The rapid increase of industrial structuring and irregular expansion of urban settlement gives rise to mixed regions where industrial facilities and housing zones are too close. Increase in industry and urbanization decreases the quality of air and is threatening human health in many ways. Particulate Matter (PM) of natural and anthropogenic origin dominates the health effects of air pollution in addition to its effects on the energy balance of the Earth-atmosphere system [1]. Air pollution has been estimated to be the cause of approximately two million premature deaths worldwide per year [2]. Particles, which are less than 10 µm in diameter (PM10), can cause serious health problems. The European Union daily average PM10 limit value is 50 µg m^{-3} [3]. *In situ* observations, representing point measurements, are usually used to determine PM mass concentrations. The samples are characterized for their chemical and physical properties. Air pollution forecast is an important issue for air quality management in cities, such as an air pollution warning system. Hence, high resolution Numerical Weather Prediction (NWP) model outputs are becoming valuable products [4].

In the literature, it has been shown that satellite remote sensing has great potential for deriving indirect estimates of ground PM, since satellite observations offer a wider spatial view than *in situ* data collections [5-9]. Remote sensing is a beneficial method for linking the results of the air pollution simulation models and analytical observations [10]. As indicated in the literature, remote sensing data and techniques are a good way of obtaining spatial distribution maps [11, 12]. With the use of values that were derived for a distribution map, it is possible to obtain data for the points of sample measurements being not available.

Many international organizations, such as European Environment Agency (EEA) and World Meteorology Organization (WMO), use satellite remote sensing techniques with *in situ* measurement and deliver information on air quality [13]. In this study, for examination of PM10 values, remote sensing techniques were used. Izmir City was selected as the study area. As a rapidly developing and populated country, many of the residential areas in Turkey are built without consideration of professional and detailed urban planning. In the city of Izmir, which is an important commercial centre located in the western part of Turkey, the impacts of unplanned urbanization and industry can be observed. The air quality of Izmir can be defined as above health risk limits. The daily average and 95th percentile of PM10 data values recorded since 2010 are 52 μg m^{-3} and 110 μ gm^{-3}, respectively.

The PM10 values were collected from the 6 stations of Izmir, and used as air quality parameter data. Landsat 5 TM images, acquired on 2 different dates (19.02. 2010 and 26.03. 2011), were used to determine the distribution of PM10 levels for the study area. These dates of satellite images were selected from the periods with high and low observed PM10 levels, respectively. The aim of the proposed method used in the current study can be summarized in four steps. The images were: i) radiometrically corrected by calculating Top of Atmosphere Reflectance (TOA), ii) atmospherically corrected by using Atmospheric & Topographic Correction (ATCOR) tool, independent from each other, iii) after obtaining resultant data, image subtraction was applied and the difference image was considered as consisting of values that represent the effect of air pollution, and iv) Optimum Band Ratio (OBRA) method, which produced all possible band ratio (BR) combinations of corresponding spectral data analyzed with target topic's data [14, 15] was then applied to difference images to get the most appropriate band combination that shows the highest correlation with PM10 values of *in-situ* air quality stations. Following this step, the regression model generated with the highest correlated BR was used to produce PM10 distribution maps of the study area.

2. MATERIALS AND METHODS

2.1 Study area

Izmir is located in the western part of Turkey, within the coordinates of 37°45' - 39°15' NW and 26°15' - 28°20' SE (Fig. 1). It has an area of 12,012 m^2 [16]. Izmir, with its 8500 years of history, and its natural beauty, has very significant touristic potential and capacity [17]. Situated by the gulf, its boundaries extend along the Gediz River's delta in the north, an alluvial plain created by several small streams in the east and a slightly more rugged terrain in the south. On the west, there is a shore of the Aegean Sea. The port of a large hinterland extending from Canakkale to Fethiye, Izmir is a very significant transportation centre. In addition, it is important for the industry, and accounts for 9.3% of total production. Agriculture-based industries are well developed and dependent on wide fertile agricultural lands. Among various types of activities that contribute to Izmir's economy, the main domains are industry (30.5%), trade and related services (22.9%), transportation and communication (13.5%), and agriculture (7.8%) [17]. Izmir, the second largest commercial centre in the country, is one of the driving forces behind Turkey's economy [17].

Izmir has an Aegean-type Mediterranean climate with 300 sunny days per year [16]. Summers are generally hot and arid, while winters are mild to cool and rainy [16]. Temperature averages (T_a) are between 30 and 36 °C during summer months, and between 10 and 16 ºC during winter months. The long-years average temperature is 17.9 ºC [16]. The long year's annual average of total precipitation for Izmir is 689 mm [17]. Average wind velocity is 3 m/s. The long-years monthly average of relative humidity (RH) is highest in December with 70%, and lowest in July with 50% [18].

According to the Turkish Statistical Institute (TSI), Izmir's population is nearly four million (2012 data), and public health is an important issue for metropolitan cities with a large population such as Izmir. It can also cause a country's economy to stagnate due to the huge costs associated with health damage [2]. In recent years, the high levels of air pollution have been highlighted in the media.



FIGURE 1 – Izmir, Study area.

2.2 Data used

2.2.1 Satellite data

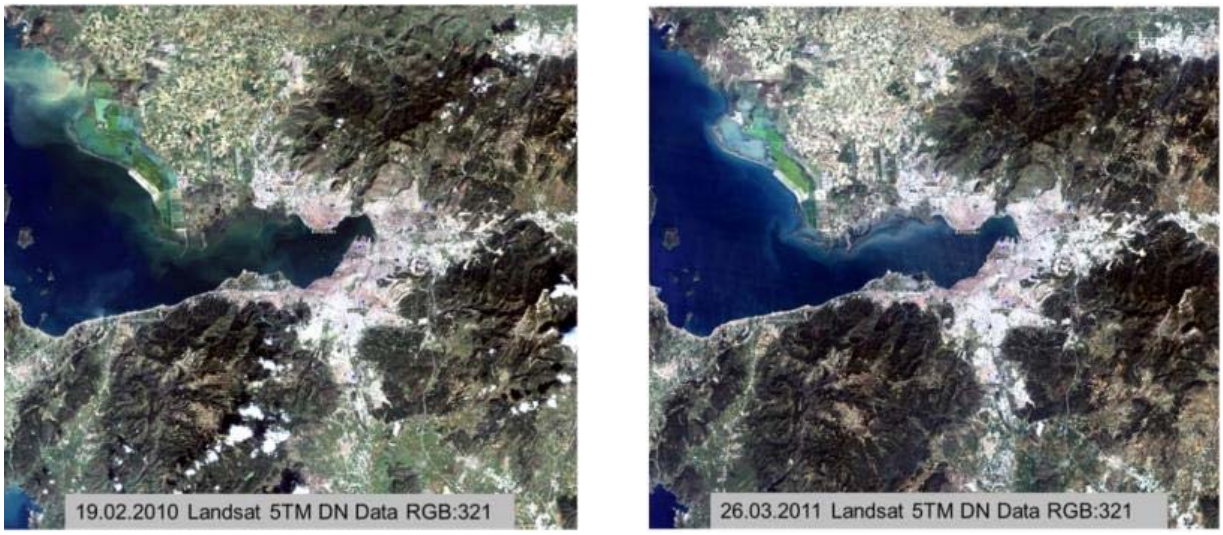
Landsat 5 Thematic Mapper (TM) imagery was used in the analysis. Landsat 5 satellite, with its circular, sun-synchronous, near-polar orbit at an altitude of 705 km, has provided digital earth images, since it was launched in 1984. Thematic Mapper sensor provides images with seven spectral bands including one thermal band. Spatial resolution is 30 m for reflective and 120 m for thermal bands. Landsat 5 TM image frames represent 170 x 185 km of earth surface. Electromagnetic portions sensed by Landsat TM acquisitions are given in Table 1. The Landsat 5 TM data used were acquired on 19 February, 2010 and 26 March, 2011 (Fig. 2).

TABLE 1 – Landsat 5 TM image specifications.

Band	Wavelength	Spatial Resolution
Band 1	(0.45 - 0.52 µm)	30 m
Band 2	(0.52 - 0.60 µm)	30 m
Band 3	(0.63 - 0.69 µm)	30 m
Band 4	(0.76 - 0.90 µm)	30 m
Band 5	(1.55 - 1.75 µm)	30 m
Band 6	(10.40 - 12.50 µm)	120 m
Band 7	(2.08 - 2.35 µm)	30 m

2.2.2 In-situ data

The study was performed by considering all hourly PM10 air quality data scanned for the dates between 01.01. 2010 and 31.12. 2012, and a selection between the dates when Landsat images were available. For determining the



(a) (b)

FIGURE 2 – Landsat 5 TM DN data of Izmir on (a) 19.02. 2010, and (b) 26.03. 2011

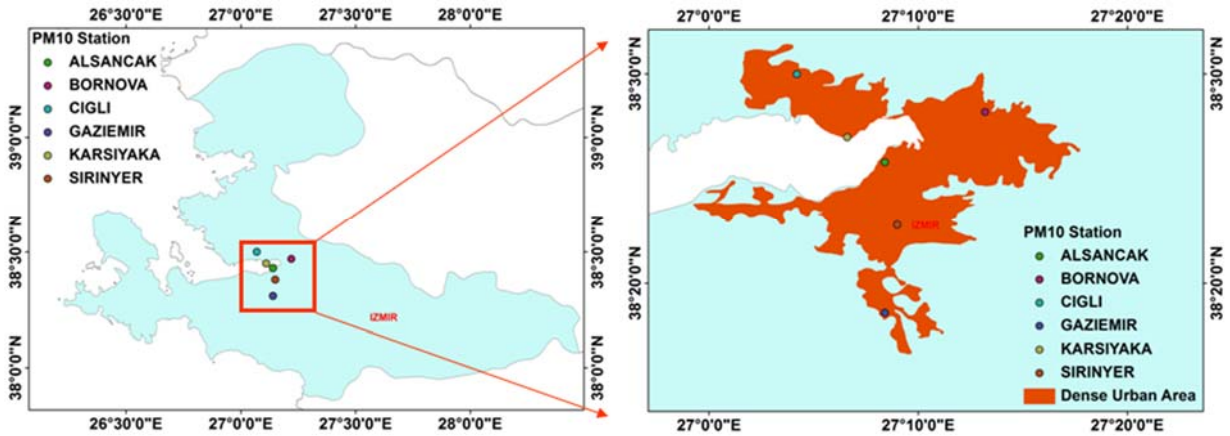


FIGURE 3 – Locations of stations.

difference between the most clear and dirty atmospheric conditions, measurements of all stations were evaluated, and the dates of measurements at extreme (i.e. low and high) PM10 values were used. The hourly PM10 values on the dates of satellite acquisitions (19.02. 2010 and 26.03. 2011) were obtained from the air quality measurement stations in Alsancak, Bornova, Cigli, Gaziemir, Karsiyaka, and Sirinyer districts. The mean of PM10 data between 09.00 and 11:00 am were generated to associate with Landsat 5 TM satellite images that had been achieved approximately at 10:40 am. The locations of stations are shown in Fig. 3. In this study, the stations that provide PM10 data were not homogeneously distributed within the city boundaries, since data records of all stations were not available. It can be said that the measurement points mainly represent the dense urban area. This was considered as an advantage, since the air pollution in the urban area was the focus of the study.

The statistical values of PM10 data during 2008–2012 for Izmir metropolitan are given in Table 2. In Table 3, the average and maximum PM10 values for each station are given with the date of measurement. The PM10 values of the stations, on both satellite data acquisition dates, are given in Fig. 4.

2.2.3 Environment - high resolution limited area model application

Environment - High Resolution Limited Area Model (Enviro-HIRLAM) is an online integrated Numerical Weather

TABLE 2 – The statistical values of PM10 during 2008–2012 for Izmir metropolitan.

Stations	0.95%	0.75%	Average	0.25%	0.05%
Alsancak	113.0	58.0	50.3	31.0	21.0
Bornova	91.0	57.0	46.4	31.0	17.0
Cigli	98.0	60.0	50.2	34.9	20.9
Gaziemir	114.8	67.0	54.8	36.0	18.2
Karsiyaka	103.0	55.0	47.4	30.0	18.0
Sirinyer	126.0	67.0	59.4	41.0	27.8
Average	*107.6*	*60.7*	*51.4*	*34.0*	*20.5*

TABLE 3 – The average and maximum PM10 values with the date of measurement, for each station.

	Alsancak	Bornova	Cigli	Gaziemir	Karsiyaka	Sirinyer
Average PM10 ($\mu g/m^3$)	44	47	47	51	45	58
Maximum PM10 ($\mu g/m^3$) (Date of sampling)	241 (12.02. 2011)	295 (27.11. 2012)	194 (01.11. 2011)	198 (12.02. 2011)	344 (14.08. 2012)	253 (12.03. 2011)

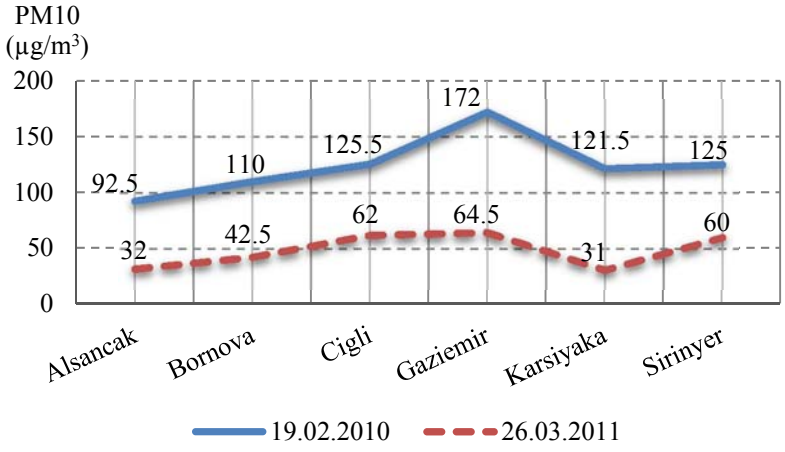
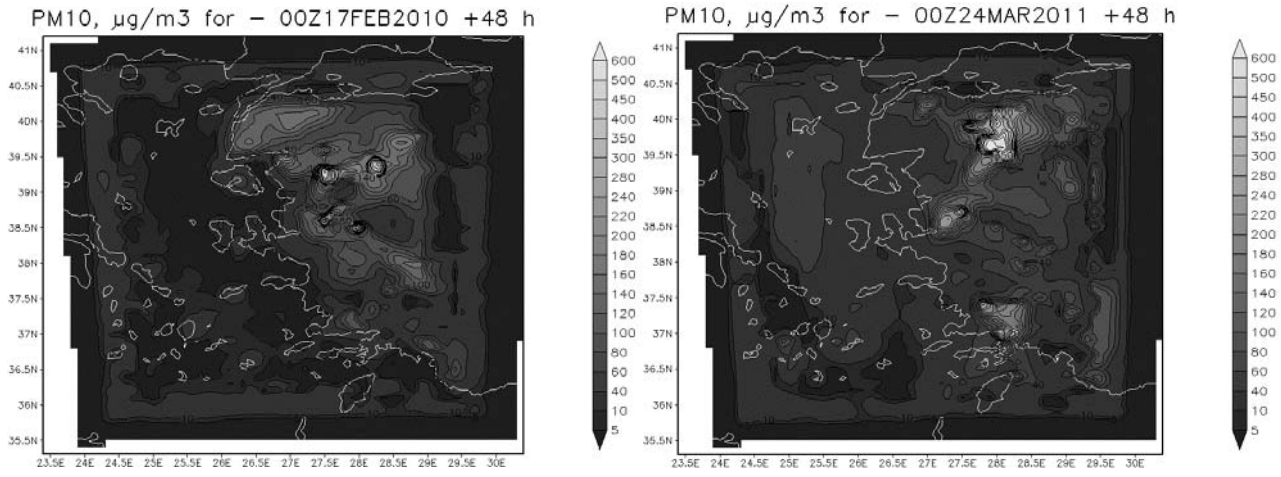


FIGURE 4 – PM10 values measured at the stations.

Prediction and Atmospheric Chemistry Transport Model (NWP-ACTM). Enviro-HIRLAM model enables simultaneous utilisation of all meteorological fields with emission, transport, mixing and chemical transformation of trace gases and aerosols [19, 20]. The Enviro-HIRLAM V7.2 has been applied to estimate PM10 content in Izmir region for two different periods. The model was run at the Istanbul Technical University (ITU) server by using the ECMWF analysis data. The model's main characteristics, features of numerics, physics analysis, and the values used in initialisation for the case study are given in Table 4. The domains are illustrated in Fig. 5 that shows the PM10 distribution over the west of Turkey. The Enviro-HIRLAM process was initialised at 00Z for 15.02. 2010 and 22.03. 2011with 48-h forecast, every 12 h for 5 days.

TABLE 4 – Summary of the Enviro-HIRLAM model setup.

Model Parameter	Value
Model version	7.2
Horizontal resolution (km)	10x10
System of coordinates	Rotated lat/lon
Nodes in x, y and z (lon, lat, lev)	54, 59, 40
Coordinates of modelling domains (lon; lat)	-5.507S,-4.017W,0.293N,1.283E
Coordinates of south pole	-49.00;28.80
Number of passive boundary points, boundary zone	2;8
Number of halo-zone points in grid-point model	6
Dynamics time step fc (s)	360
Climate data set projection	9000
Resolution of climate data sets (as per available)	0.0125
Dynamics	Hydrostatic
Physics	HIRLAM
Land surface scheme	ISBA
Boundaries	ECMWF(25km)
Activate tracers in forecast scripts	Yes (AEROSOLM7)
Activate anthropogenic emissions (TNO)	Yes
Activate biogenic emissions (Dust, Sea-Salt, Isoprene)	Yes
Activate dry and wet deposition for aerosols and gases	Yes
Activate direct and indirect aerosol effects	No
Use mass-conserving LMCSL-scheme for advection	Yes
Meteorological variables (Q,S,SVAR(1:2)	Yes
Data assimilation analysis	No



(a) (b)

FIGURE 5 – Model domain for 17.02. 2010 (a), and 24.03. 2011 (b).

2.3 Application

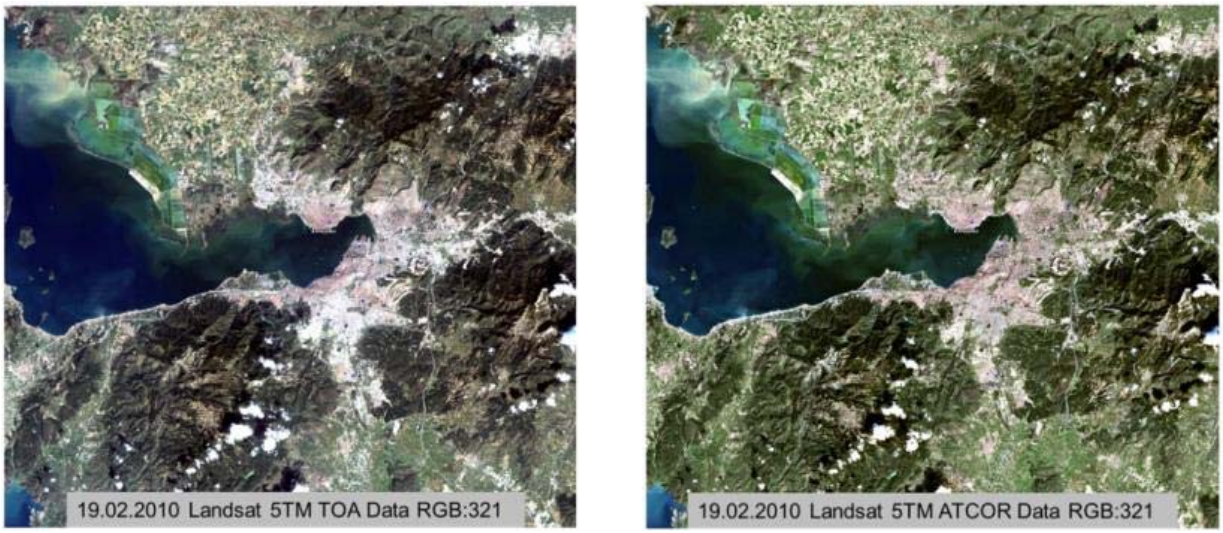
As a first step, two independent data were produced as TOA corrected and ATCOR corrected images. Then, band math was applied to get a difference image of them. By using OBRA method, all possible BR combinations were generated, and the most appropriate band combinations possessing the highest correlations with PM10 values of air quality stations were obtained. The direct pixel value of the station may not give the highest correlation with station data, because the air is extremely fluid causing rapid transportation of the pollutants. Therefore, the filter size, which best matches the amount of the PM10 values, was investigated. The steps of application are as follows:

1. Two separate operations were applied to the Landsat images: i) Images were radiometrically corrected by the calculation of Top of Atmosphere (TOA) reflectance. After this operation, the images consisted of the data representing TOA values; ii) Images were atmospherically corrected by using ERDAS Imagine software's ATCOR tool algorithm. By using this operation, the effects of haze, vapor, aerosol particles, atmospheric distortion, solar illumination and shadowing were removed/reduced. The obtained data represent the atmospherically corrected values.

Figure 6 shows the images obtained after applying TOA (a) and ATCOR (b) operations, for the 19.02. 2010 dated image, and Fig. 7 shows the images obtained after applying (a) TOA and (b) ATCOR operations, for the 26.04. 2011 dated image.

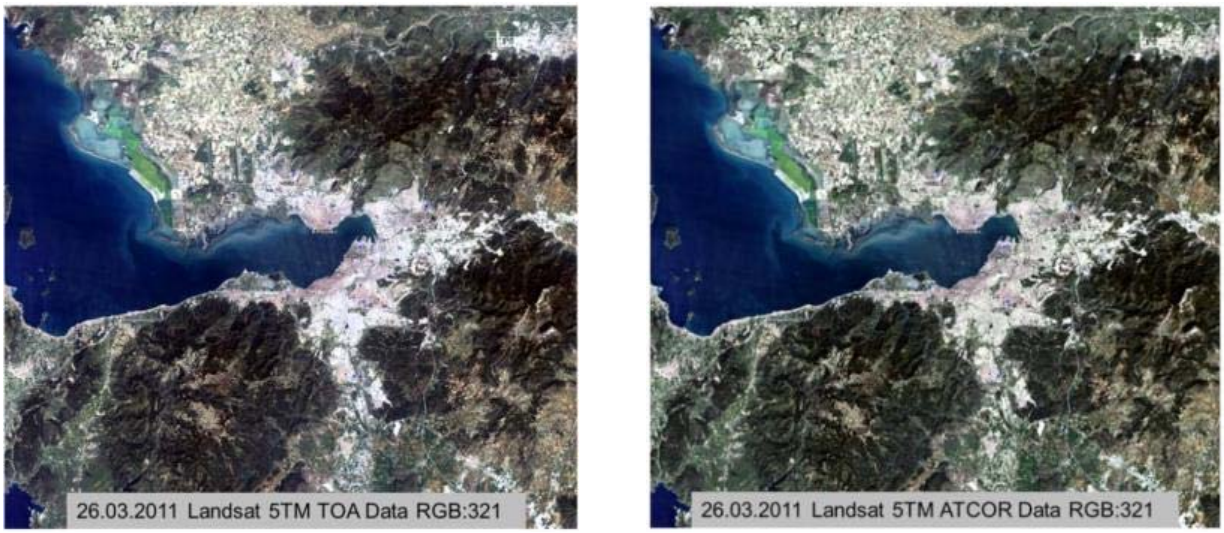
2. The difference image was produced by subtracting the atmospherically corrected image data from the top of atmosphere data, by using Equation 1. The result images are given in Fig. 8 for (a) 19.02. 2010 and (b) 26.03. 2011.

$$Difference\ image = TOA\ DATA - ATCOR\ DATA \quad (1)$$



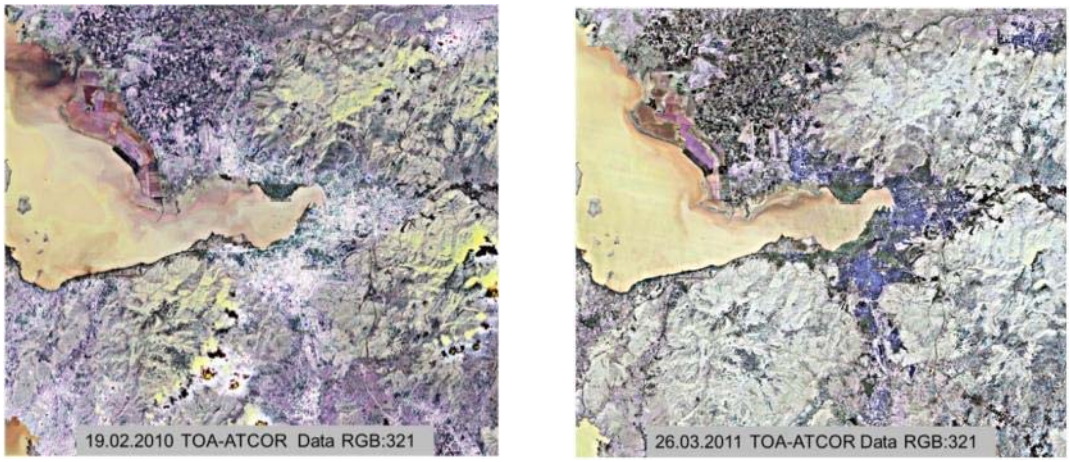
(a) (b)

FIGURE 6 – (a) TOA data (b) ATCOR data for the 19.02. 2010 dated image.



(a) (b)

FIGURE 7 – (a) TOA data, and (b) ATCOR data for the 26.03. 2011 dated image.



(a) (b)

FIGURE 8 – Difference image of (a) 19.02. 2010, and (b) 26.03. 2011 dated data.

3. Taking OBRA method as the basis, in this study, all possible band ratio (BR) index values were calculated using difference images. The BR index values were performed by using Equation 2:

$$BR(x,y,i)=\left\{\frac{R_x(\lambda_1)}{R_x(\lambda_2)}\right\}\begin{matrix}Band\,1\le\lambda_1\le Band\,7\\ Band\,1\le\lambda_2\le Band\,7\end{matrix}\quad 1\le i\le(number\,of\,sample\,(6)) \qquad (2)$$

where, BR = band ratio, R = reflectance, I = number of sample (i.e. stations = 6), and λ = Landsat band.

To determine the most appropriate BR, all possible BR images and PM10 values were correlated. The operation was conducted for the direct pixel value, which is exactly at the location of the PM10 station, and repeated for mean filter values of 3x3, 5x5, 7x7, 9x9 and 11x11 image windows. In this way, both the best correlation and the best filter size to represent the PM10 were investigated.

4. The highest correlation BR was used to produce PM10 distribution maps.

5. Finally, the findings were interpreted with the outputs of Enviro-HIRLAM model.

RESULTS

The correlation coefficient values (r) were calculated for all image filter sizes (1x1 (direct pixel), 3x3, 5x5, 7x7, 9x9 and 11x11) of all possible BR combinations. In Table 5, the highest positive (HP) and highest negative (HN) r values, and the related BR indices are given.

For difference images of 19.02. 2010 and 26.03. 2011, the following results were obtained:

Band 5/Band 7 (B5/B7) and B7/B5 were found to be mostly and commonly correlated with PM10, except 1x1 and 11x11. However, the results of B5/B7 were presented to make the presentation of the paper concise.

As it can be seen in Table 5, the mean filter sizes of 3x3 and 7x7 provide very close correlation results with PM10. On the other hand, in comparison with 7x7 (7x30 = 210 m)x(7x30 = 210 m), 3x3, which is the mean of (3x30 = 90 m)x(3x30 = 90 m), ensures high details and spatial resolution. Accordingly, due to the advantages of 3x3, 3x3 was selected rather than 7x7.

The scatterplots for each filter (i.e. window) size of HP results are given in Figs. 9 (a-f). The slope and intercept of regression line and r are given in the plots.

It was determined that the higher correlations between PM10 and BR indices can be obtained under high PM10 content conditions, as 19.02. 2010 correlations were superior to those of 26.03. 2011. These results indicated that the higher PM10 values, the higher the correlation between the values and satellite derived data (i.e. difference image) are. This seems to be based on the reality that the method runs on the difference image of the atmospherically corrected and non-corrected images. In other words, if the difference

TABLE 5 – HP and HN correlation values (r) and band ratios (BR).

Date	r Type	1x1		3x3		5x5		7x7		9x9		11x11	
		r	BR	r	BR	R	BR	r	BR	r	BR	r	BR
19.02. 2010	HP	0.98	B5/B7	0.86	B5/B7	0.88	B5/B7	0.89	B5/B7	0.83	B5/B7	0.71	B4/B6
	HN	-0.98	B7/B5	-0.82	B7/B5	-0.86	B7/B5	-0.87	B7/B5	-0.83	B7/B5	-0.75	B6/B4
26.03. 2011	HP	0.59	B4/B7	0.86	B5/B7	0.83	B5/B7	0.83	B5/B7	0.86	B5/B7	0.86	B5/B7
	HN	-0.59	B7/B4	-0.90	B7/B5	-0.86	B7/B5	-0.86	B7/B5	-0.88	B7/B5	-0.87	B7/B5

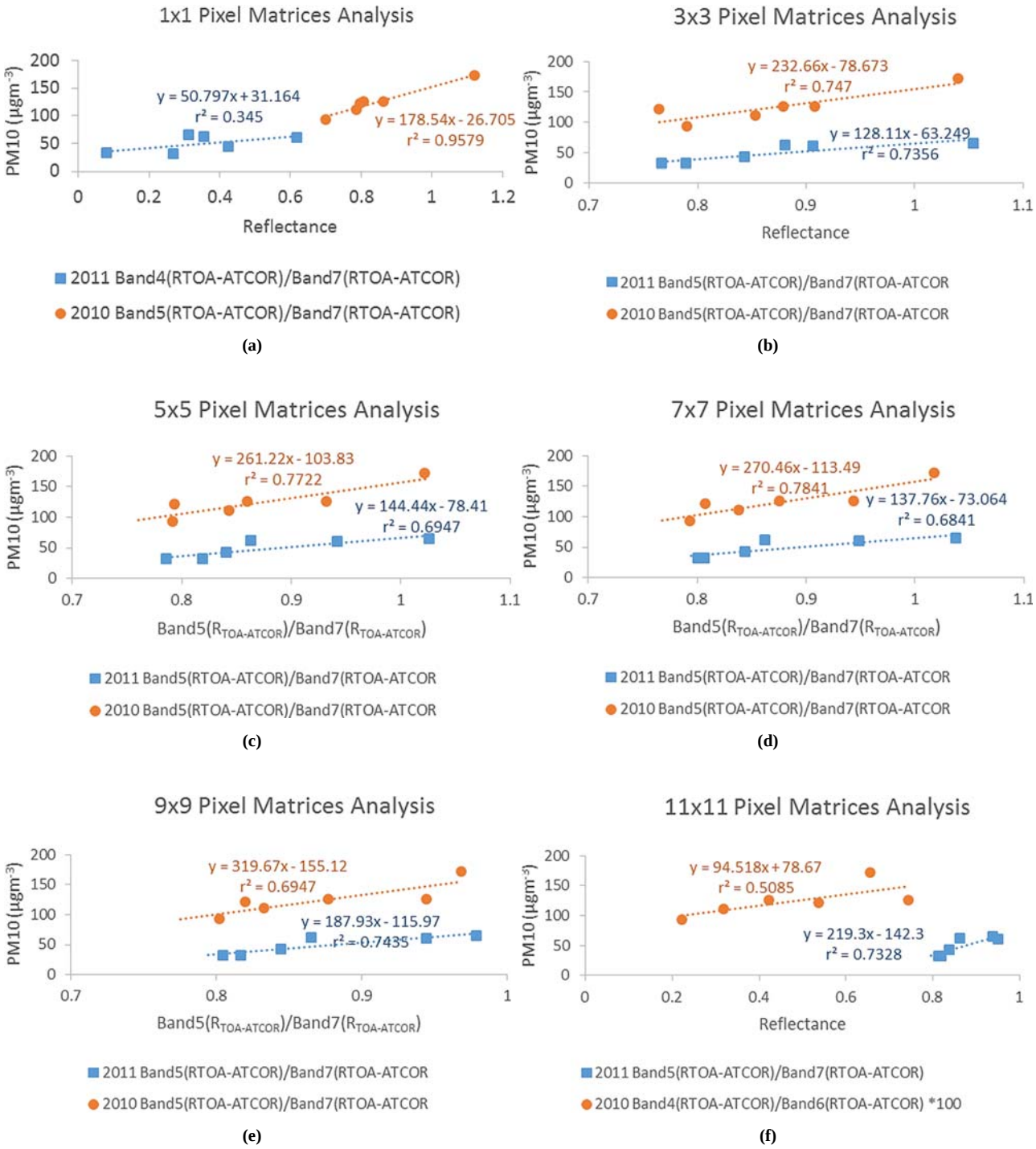


FIGURE 9 – Scatterplots of HP correlation and regression analysis for (a) 1x1, (b) 3x3, (c) 5x5, (d) 7x7, (e) 9x9, and (f) 11x11 window sizes.

is high, it indicates that the PM10 level of the point is high. PM10, which is a type of aerosol, works as condensation nucleus, and the water vapor in the atmosphere condensates over aerosols [21]. In high moisture areas, especially such of coastal regions, high PM10 levels increase cloud formations. As is known, the reflectance values in the infrared (IR) portion of the electromagnetic spectrum are relational with cloud temperature [22]. Thus, the findings of the study seem to be meteorologically significant.

According to the findings explained till here, briefly, there are higher correlations than calculated for 3x3 window. However, notably, the common determined filter size of the high correlations for both of the dates is 3x3, which

is the data of 90 m^2, with the BR = B5/B7. After obtaining the regression equations, the PM10 distribution maps were created. For this process: i) the 3x3 filter images were prepared, ii) B5/B7 index images were produced, iii) equations 3 and 4 were used to convert the index images into PM10 values for 2010 and 2011 dates, respectively:

$$PM10 = 232.66x\left(B5/B7\right) - 78.673 \quad (3)$$

$$PM10 = 1281.11x\left(B5/B7\right) - 63.249 \quad (4)$$

The results indicated the same unit (μg/m^3) for PM10 as measured by the air quality stations. The produced map gives the derived PM values over a wide and dense urban area (Fig. 10).

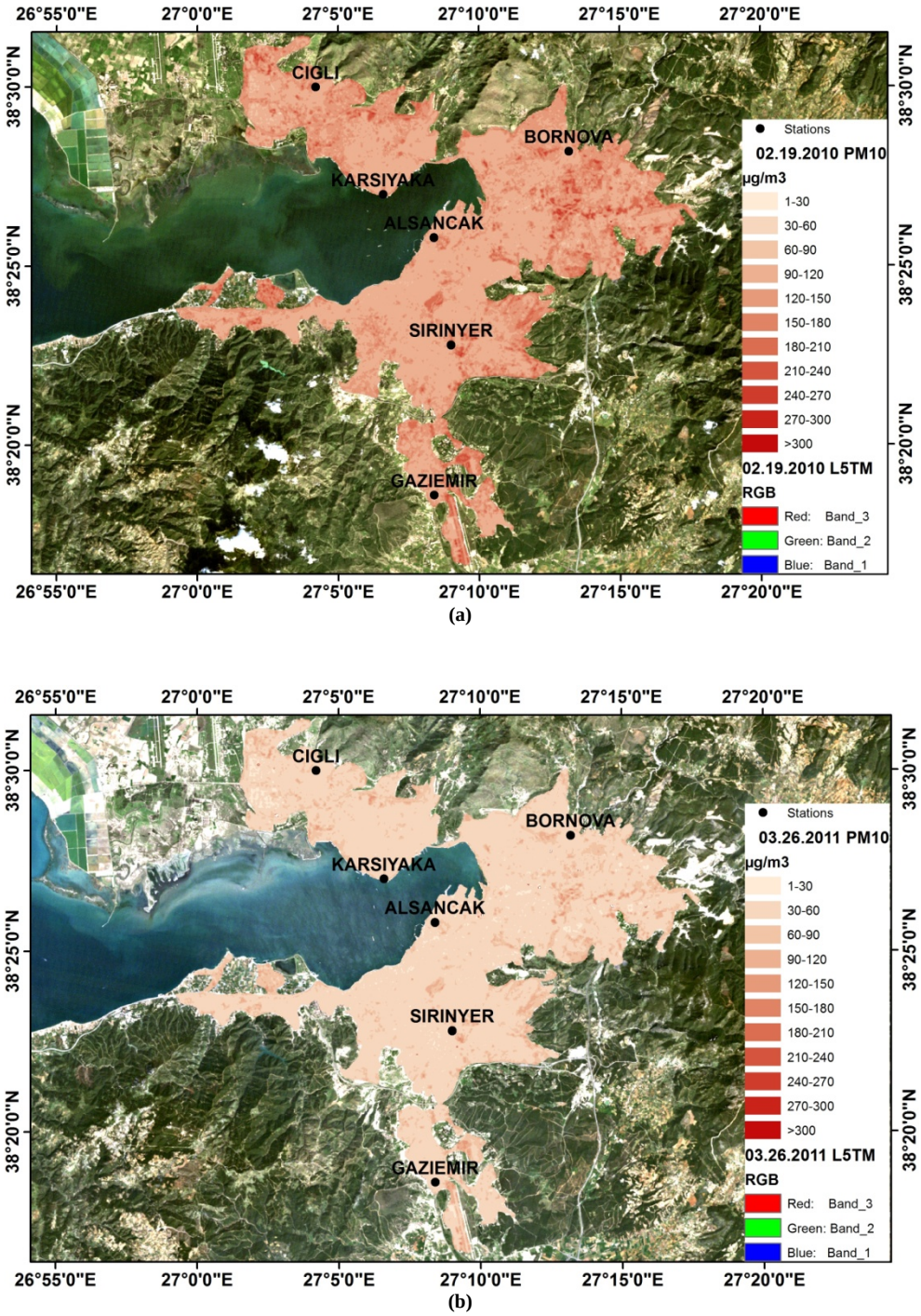


FIGURE 10 – PM10 distributions for (a) 02.19. 2010, and (b) 03.26. 2011 dates.

The usability of the map was investigated by evaluating the map and the reality. It is obvious, from the visual analysis that, in February 2010, the values are higher than the values in March 2011, which shows that the pollution was denser. In 2010, much more air pollution is observed in Bornova region, where there is more industrialization than in other districts. The values seem to be higher than expected, such as 270 and even 300 μg/m^3. However, this is more than the maximum PM10 values measured for 19.02. 2010 and 26.03. 2011. To evaluate the accuracy or approximation of derived values, the study region was analyzed. Particularly, at points near very busy streets or points very close to pollutants, the limits are exceeded [23]. In Bornova, there is a significant irregular urbanization with shanty settlements, industrial zone and a highway crossing the centre. When the PM10 values other than the image acquisition dates were searched for, high values were found that were measured *in situ* for later than January 2010, as can be seen in Table 2. One of the reasons for critical levels may be the increase in gas and fuel consumption in the winter months that has impact on air pollution. The values seem to be high on some summer days, as can be seen on 14 August, 2012. The possible reasons may be high humidity, which can keep the particles in the air, in addition to the low wind velocity that may be caused by the protected land geography and topography of the area. The topographic structures of Izmir may trigger air pollution. However, these suggestions and their relation to the meteorology have to be investigated. According to the weather report for February 17th, 2010, a low pressure system was built over the Southeast on that day. This might have resulted as cloudy weather on the following day. In addition, a cyclone brought warm moist weather from the Southwest to Izmir Area. According to the weather report for March 24th, 2011, atmosphere was causing cold moist weather from the Northwest.

The Enviro-HIRLAM 45h forecasts for 19.02. 2010 and 26.03. 2011 are given in Figs, 11 and 12. The maximum PM10 was approximately 110 and 20 μg/m^3 for 19.02. 2010 and 26.03. 2011, respectively. There was a source of pollution near Izmir city centre as can be seen in the figures. The Enviro-HIRLAM model forecast for two different days gave a good signal for more and less polluted days. The model result resolution is too low to be compared with sample collection grid and spatial resolution of satellite images. This result may depend on city emission inventories. This may be the scope for further studies analysing the model at high resolution.

Both HIRLAM and remote sensing results showed that on February 2010, air quality was worse than on March, 2011. In this context, model and OBRA based remote sensing method gave consistent outputs. The output of remote sensing analysis is not represented as homogeneous and smooth as model outputs, because the resolution of satellite images is higher; on the contrary, the discontinuous form may well represent the point source pollutants caused by land-use and land-cover of the area, at a rate of spatial resolution of the satellite image.

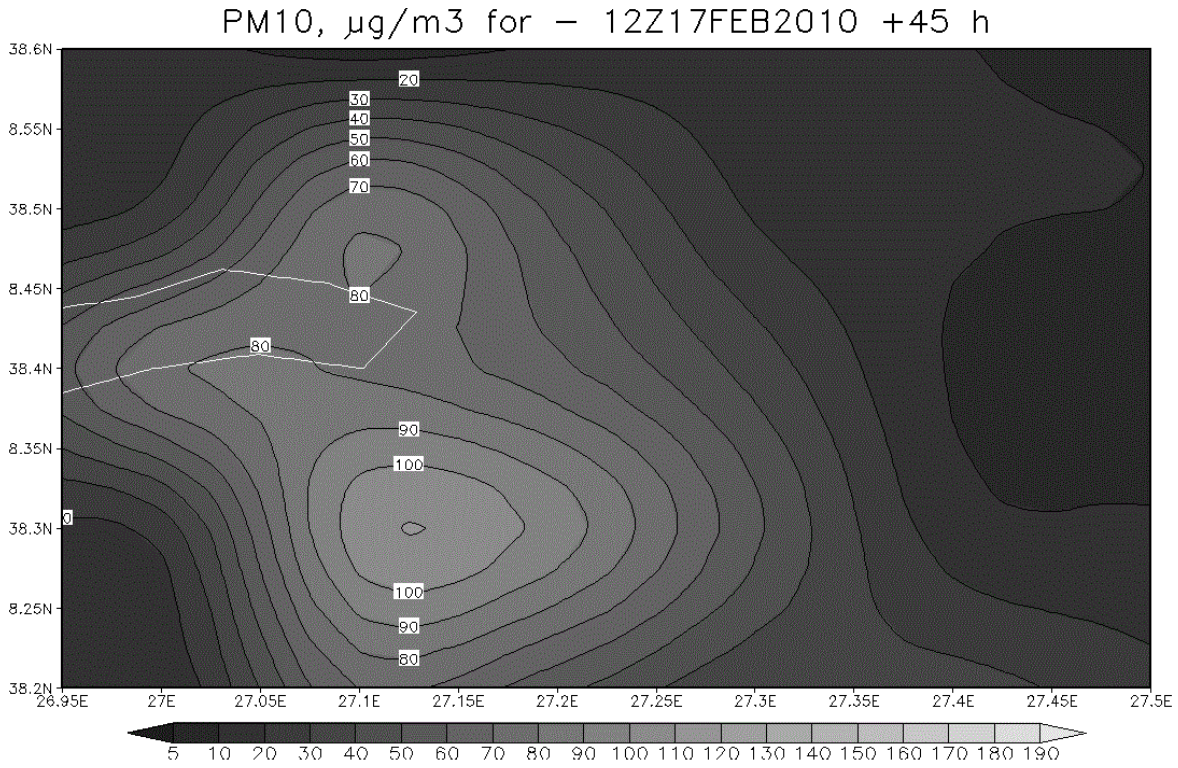


FIGURE 11 – The 45-h forecasts produced by the Enviro-HIRLAM model for 09Z, 19 February 2010.

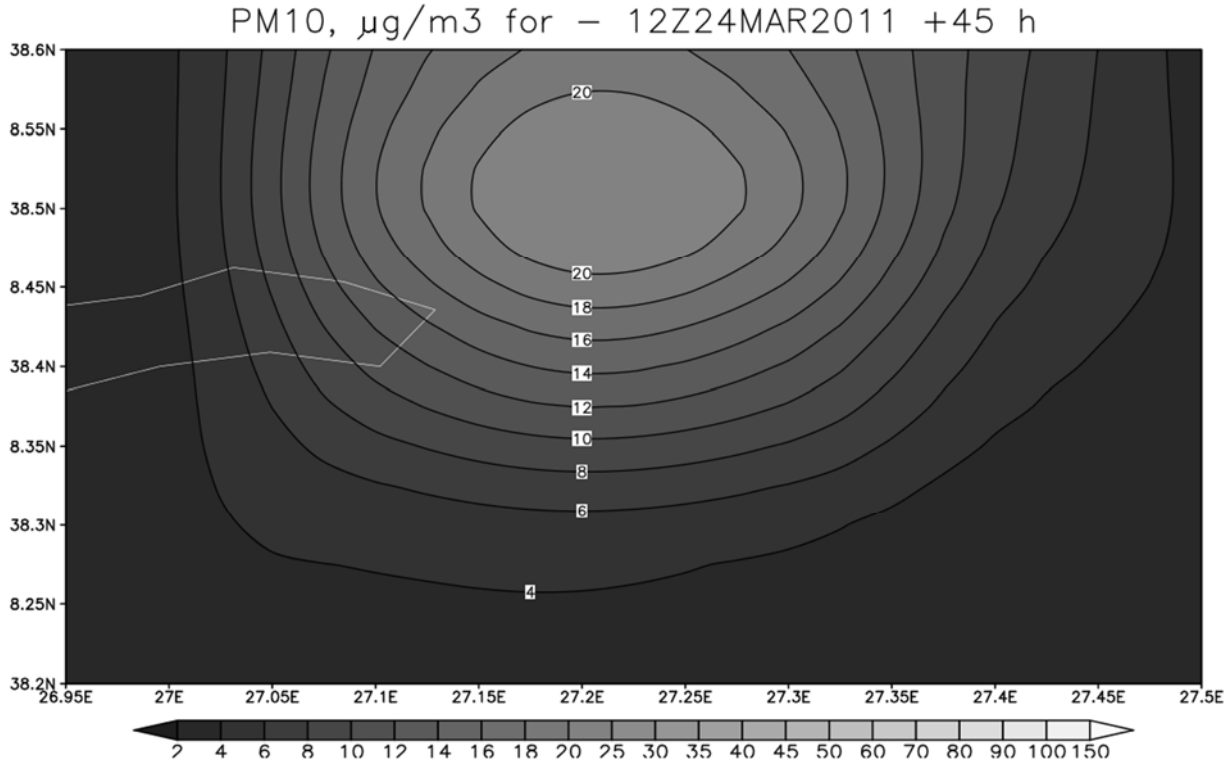


FIGURE 12 – The 45-h forecasts produced by the Enviro-HIRLAM model for 09Z, 26 March 2011.

4. CONCLUSIONS AND RECOMMENDATIONS

The observed PM10 values are beyond human health risk levels. The people living in this region, especially children and the elderly, have to be aware of air pollution, and protect themselves by staying indoors or wearing masks according to the air quality situation.

Although our study is an initial step and a case study, the results are satisfactory and promising. All determined correlation levels are in a strong and very strong relationship class. Finally, the method used is easy, practical, and feasible for monitoring air quality. As a further study, the PM10 distribution maps can be integrated to a geographical information system and analyzed with relational data (such as air pollution-related illness distributions) in order to obtain more reliable interpretations to act against air pollution effects.

Furthermore, multi-temporal analysis can be performed for various locations. The results of this initial study are site-specific and, therefore, they cannot be generalised. However, the study can be enhanced by applying the same method to different types of land-use/land-cover regions, since separately analysing the behaviour of different aerosol models used in different atmospheric correction methods can be effective to get more accurate results. In future studies, the number of dates under investigation may be increased, the air quality in different cities can be evaluated, the different classification techniques can be tested, and different types of satellite images can be examined to find the most appropriate method for determination of air pollution using remote sensing techniques.

ACKNOWLEDGMENT

The authors would like to thank the Ministry of Environment and Urbanism of Turkey for the air quality data. This work was part of the Turkish Scientific and Technical Research Council (TUBITAK) Project No: 111Y319.

The authors have declared no conflict of interest.

REFERENCES

[1] Dinoi, A., Perrone, M. R., Burlizzi, P. (2010) Application of MODIS Products for Air Quality Studies over Southeastern Italy. Remote Sens., 2, 1767-1796; doi:10.3390/rs2071767.

[2] Yap, X. Q., Hashim, M., and Marghany, M. (2011) Retrieval of PM10 Concentration from Moderate Resolution Imaging Spectroradiometer (MODIS) derived AOD in Peninsular Malaysia, IGARSS, 2011, 4022-4025.

[3] De Leeuw, F. and Ruyssenaars, P. (2011) Evaluation of current limit and target values as set in the EU Air Quality Directive. ETC/ACM (The European Topic Centre on Air Pollution and Climate Change Mitigation), Technical Paper 2011/3. https://www.eionet.europa.eu/events/EIONET/ETC_ACM_Report

[4] Toros, H., Geertsema, G., and Cats, G. (2014) Evaluation of the HIRLAM and HARMONIE numerical weather prediction models during an air pollution episode over Greater İstanbul Area. CLEAN - Soil, Air, Water, 42, 7, 863–870. doi:10.1002/clen.201200306.

[5] Gupta, P., Christopher, S.A. (2008) Seven year particulate matter air quality assessment from surface and satellite measurements. Atmos. Chem. Phys., 8, 3311-3324.

[6] Schaap, M., Apituley, A., Timmermans, R.M.A., Koelemeijer, R.B.A. and De Leeuw, G. (2009) Exploring the relation between aerosol optical depth and PM2.5 at Cabauw, the Netherlands. Atmos. Chem. Phys., 9, 909-925.

[7] Tsai, T.C., Jeng, Y. J., Chu, D. A., Chen, J.-P., and Chang, S.-C. (2009) Analysis of the relationship between MODIS aerosol optical depth and particulate matter from 2006 to 2008. Atmos. Environ.; doi:10.1016/j.atmosenv.

[8] Sarigiannis, D.A., Gotti, A., Tombrou, M., Dandou, A., Protonotariou, A., Sifakis, N.I. (2004) Comparison of data fusion methods for satellite-assisted determination of PM10 ambient concentration, Proceedings of SPIE - The International Society for Optical Engineering 5571 , art. no. 32 , pp. 282-292.

[9] Sarigiannis, D.A., Gotti, A., Sifakis, N.I., Schaefer, K., Tombrou, M. and Soulakellis, N. (2005) High precision measurement of fine and ultra-fine particles using satellite data, Symposium on Air Quality Measurement Methods and Technology.

[10] Sarigiannis, D.A, Soulakellis, N.A. and Sifakis,N.I. (2004) Information fusion for computational assessment of air quality and health effects. Photogrammetric Engineering & Remote Sensing, 70(2), February 2004, pp. 235–245.

[11] Musaoglu, N., Seker, D. Z., Kabdasli, S., Kaya, S. and Duran, Z. (2004) Using remote sensing and GIS for the assessment of visual attributes; case study of the south coastal zone of Turkey. Fresenius Environmental Bulletin, 13(9), 854-859.

[12] Kaya, S., Seker, D. Z. and Tanik, A. (2012) Analysis of urbanized areas using V-I-S components model. Fresenius Environmental Bulletin, 21(11), 3243-3248.

[13] German Aerospace Center, Promote Final Report Atmosphere. Retrieved October 17, 2010 from http://www.gse-promote.org/docs/FinalReport_WebVersion.pdf..

[14] Legleiter, C. J., Roberts, D. A., Marcus, W. A. and Fonstad, M. A. (2004) Passive optical remote sensing of river channel morphology and in-stream habitat: Physical basis and feasibility", Remote Sensing of Environment 93, 493–510.

[15] Legleiter, C. J., Roberts D. A. and Lawrence, R. L. (2009) Spectrally based remote sensing of river bathymetry, earth surface processes and landforms, Earth Surf. Process. Landforms 34, 1039–1059.

[16] Web page of Izmir Metropolitan Municipality, İzmir City Booklet: http://www.izmir.bel.tr/booklet/online_brosur_ingilizce/Default.html (Accessed on December, 2013)

[17] Web page of Turkish State Meteorological Service: http://www.mgm.gov.tr/veridegerlendirme/il-ve-ilceler-istatistik.aspx?m=IZMIR (Accessed on December, 2013)

[18] Web page of Governorship of Izmir: http://www.izmir.gov.tr/default_b0.aspx?content=216 (Accessed on December, 2013)

[19] Baklanov, A. (2008) Integrated Meteorological and Atmospheric Chemical Transport Modeling: perspectives and strategy for HIRLAM/HARMONIE. HIRLAM Newsletter, 53, 68-78.

[20] Korsholm, U.S., Baklanov, A., Gross, A., Mahura, A., Sass, B.H., Kaas, E. (2008) Online coupled chemical weather forecasting based on HIRLAM – overview and prospective of Enviro-HIRLAM. HIRLAM Newsletter, 54, 151-169.

[21] Karydis, V. A., P. Kumar, D. Barahona, I. N. Sokolik, and A. Nenes (2011) On the effect of dust particles on global cloud condensation nuclei and cloud droplet number, J. Geophys. Res., 116, D23204, doi:10.1029/2011JD016283.

[22] Pierrehumbert, R.T. (2011) Infrared Radiation and Planetary Temperature. Physics Today, 64:33-38. http:// geosci.uchicago.edu/~rtp1/papers/PhysTodayRT2011.pdf.

[23] Görgen, R. and Lambrecht, U. (2007) Particulate matter in ambient air. The debate on the PM10 daily limit value. Particulate Matter in Ambient Air, JEEPL 4|2007, 278-288.

Received: February 23, 2015
Accepted: February 23, 2015

CORRESPONDING AUTHOR

Muhittin Karaman
Istanbul Technical University
Faculty of Aeronautics and Astronautics
Department of Geological Engineering
Geochemistry Research Group and Jal Laboratories
Ayazaga Campus, Maslak, Istanbul
TURKEY

E-mail: mkaraman@itu.edu.tr

FEB/ Vol 24/ No 4b/ 2015 – pages 1585 - 1596